Vietnam Journal of Mechanics, Vol. 45, No. 2 (2023), pp. 164 – 182
DOI: https://doi.org/10.15625/0866-7136/18192

FREE VIBRATION ANALYSIS OF FGM FRAMED NANOSTRUCTURES USING VARIATIONAL-CONSISTENT BOUNDARY CONDITIONS

Duong The Hung[1], Tran Van Lien[2,*], Tran Binh Dinh[2], Nguyen Tat Thang[2]
[1]*Thainguyen University of Technology, Vietnam*
[2]*Hanoi University of Civil Engineering, Vietnam*
[*]E-mail: lientv@huce.edu.vn

Received: 26 March 2023 / Published online: 14 June 2023

Abstract. This paper analyses free vibrations of framed nanostructures made of Functionally Graded Material (FGM) based on the Nonlocal Elastic Theory (NET) and the Dynamic Stiffness Method (DSM). FGM characteristics vary nonlinearly throughout the height of the beam element. The NET considers the nonlocal parameter that perfectly captured the size effect of nanostructures. However, the NET makes nonlocal paradoxes in the bending and vibration behaviour of framed nanostructures with the free ends. To overcome these phenomena, the nanostructure is modelled according to the Euler–Bernoulli beam theory and the variational-consistent nonlocal boundary conditions have been derived. The exact solutions of differential equations of motion and variational-consistent nonlocal boundary conditions are found using the DSM. The influences of the nonlocal, material, geometry parameters and Pasternak's foundation on the free vibration are then analyzed. It is shown that the study can be applied to other FGMs as well as more complicated framed structures.

Keywords: FGM, nanobeam, DSM, variational-consistent boundary conditions, nondimensional frequency.

1. INTRODUCTION

Functionally Graded Material (FGM) is an advanced composite material designed to attain numerous superior thermal and mechanical properties, thereby enhancing the functionality of numerous existing structures [1]. The FGM is widely utilised in many fields, such as aerospace technology, chemistry, automobiles, electronics, optics, biomedical engineering, nuclear and mechanical engineering and so on. Micro/nano-sized structures such as plates, sheets and beams made of FGMs are also used in MEMS/NEMS

devices to earn high sensitivity and desired performance [2–6]. Nanomechanical resonators, nanoscale mass sensors, electromechanical nanoactuators, nanoscale generators, and nanoenergy harvesters are salient examples of these NEMS-based devices.

At the macroscale, the stress tensor at a particular point is a function of the strain tensor at the same point according to classical elasticity theory. However, the classical elasticity theory is unable to consider small-size effects at the micro/nanoscale because the dimensions of the structures are equivalent to their inter-atomic distances. To address the issue, Eringen proposed Nonlocal Elasticity Theory (NET) [7], which assumes that the stress tensor depends not only on the strain tensor at one point but also on the strain tensors at all surrounding points. Nowadays, the NET is widely used to research micro/nanostructures made of homogeneous materials [8, 9] and FGM materials [10].

The governing equations to study bending, vibration and stability problems of homogeneous beams are established in [11]. Analytical and semi-analytical methods [12–17], Finite Element Method (FEM) [18–26], Differential Transform Method (DTM) [27], and Differential Quadrature Method (DQM) [28] are applied to study the bending, stability, and vibration of nanobeams made of homogeneous and FGM materials. It is worth noting that the above methods are restricted to nanobeams. For complicated nanostructures such as multi-span beams, multi-stepped beams and nanoframes, FEM is applied to analyze the bending, vibration and buckling of nanostructures. It has been observed that the Finite Element Method (FEM) is an approximation technique that relies on the selection or assumption of shape functions, regardless of the frequencies involved. Consequently, FEM may not accurately capture high frequencies and mode shapes, even with a refined element mesh and the utilization of more complex elements [29, 30]. The Dynamic Stiffness Method (DSM) is an excellent alternative method that addresses the aforementioned limitation of FEM. It achieves this by utilizing frequency-dependent shape functions derived from exact solutions of the vibration problem [31–34]. They can be justifiably regarded as exact because there are no assumptions made on route to describe the displacement field. If there are any perceived assumptions, they are within the limits of the governing differential equations of motion. Although these exact solutions are not easily found for complicated structures, in possible cases, they help us find the exact response of the structure, especially in a high-frequency range. Moreover, responses of the structure obtained from DSM are not independent of the number and selection of finite elements. Adhikari et al. [35] applied DSM to analyse the vibration of damped nanorods [20], nanorods embedded in an elastic medium [36], and damped nanobeam on an elastic foundation [37]. Recently, Taima et al. [38] used DSM to analyse the free vibration of multi-stepped FGM Bernoulli-Euler nanobeams.

Although NET is widely used to research micro/nanostructures, the NET can create some nonlocal paradoxes in the bending and vibration of nanobeams and nanoplates

[39, 40]. For example, an incorrect stiffening phenomenon happens to a fundamental frequency of nanostructures with free ends [40]. These paradoxes occur owing to the inconsistent establishment of the boundary conditions for nanostructures. These inconsistent boundary conditions are obtained by simply replacing the classical force resultants with the nonclassical force resultants in the equilibrium equations [41]. A correction of the boundary conditions is needed when applying the nonlocal model of Eringen to nanostructures with free ends. There are many proposals to solve these paradoxes such as Challamel et al. [42] proposed a discrete nanobeam model, Khodabakhshi and Reddy [43] proposed a integro-differential model. Some authors established the correct nonlocal boundary conditions using variational formulations. Zhang et al. [44] used the method of weighted residuals to obtain the boundary conditions for the buckling of nonlocal Timoshenko homogeneous beams with simply supported ends. Yan et al. [45] employed Galerkin method to receive correct nonlocal bending deflections of homogeneous nanostructures. Xu et al. [46] applied the weighted residual method to obtain the variational-consistent boundary conditions for homogeneous nanobeams. Aria and Friswell [26] utilised the weak form of equations of motion and applied FEM to analyse the vibration of FGM nanobeams. Recently, Lien et al. [47] used the weak form of the equation of motion to obtain the variational-consistent boundary conditions of the FGM Timoshenko nanobeams.

To the best of the authors' knowledge, a correction of the boundary conditions for the nonlocal FGM nanobeams and nanostructures with free ends is a gap that must be fulfilled. In this work, the variational-consistent nonlocal boundary conditions and the exact solutions of differential equations of motion of FGM Euler-Bernoulli nanobeams have been derived. This solution has overcome the nonlocal paradox of the fundamental frequency of nanobeams and nanostructures with the free ends. From there, the changes in the vibration frequencies of FGM framed nanostructures considering the material distribution profile, nonlocal effects and the Pasternak's foundation are studied. A comprehensive investigation has been conducted to study the impact of nonlocal size effects, material distribution profile, geometry, and Pasternak's foundation parameters on the vibration frequency of nanostructures with free ends.

2. A NONLOCAL FGM EULER–BERNOULLI NANOBEAM

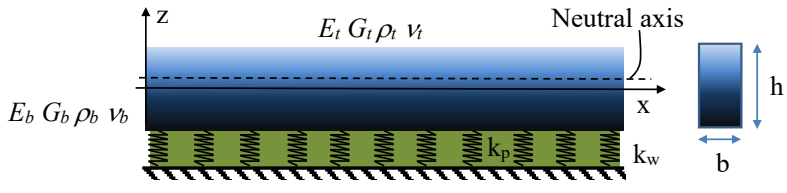

Fig. 1. A FGM nanobeam on a Pasternak's elastic foundation

A FGM beam of the length L and rectangular cross-section $b \times h$ rested on the Pasternak's elastic foundation (Fig. 1) is considered. Assuming the material properties of the FGM beam vary along the height following the power-law distribution (P-FGM) as follows [1]

$$\{P(z)\} = \{P_b\} + \{P_t - P_b\}\left(z/h + 0.5\right)^n, \quad -0.5h \le z \le 0.5h, \tag{1}$$

where P stands for modulus of elastic modulus E, shear modulus G, and mass density ρ, respectively; the subscripts t and b refer to the corresponding top and bottom layer materials; n is the power law or volume fraction index; and z is the coordinates from the mid-plane of the beam.

The displacements of the Euler–Bernoulli beam can be represented in the form as follows

$$u(x,z,t) = u_0(x,t) - (z-h_0)\, w_{0,x}(x,t), \quad w(x,z,t) = w_0(x,t), \tag{2}$$

where $u_0(x,t), w_0(x,t)$ are the longitudinal and transverse displacements of a point on the neutral axis, respectively; h_0 is the distance from the neutral axis to the x-axis. From (2), we get the strain component

$$\varepsilon_{xx} = u_{0,x} - (z-h_0)\, w_{0,xx}(x,t). \tag{3}$$

Setting

$$\begin{aligned}
(A_{11}, A_{12}, A_{22}) &= \int_A E(z)\left(1, z-h_0, (z-h_0)^2\right) \mathrm{d}A, \\
(I_{11}, I_{12}, I_{22}) &= \int_A \rho(z)\left(1, z-h_0, (z-h_0)^2\right) \mathrm{d}A,
\end{aligned} \tag{4}$$

where A_{11}, A_{12}, and A_{22} are the rigidities, and I_{11}, I_{12}, and I_{22} are the mass moments, respectively. Ignoring the influence of the nonlocal parameter and axial displacement, Eltaher [24] determined the neutral axis position from the condition that the axial force at the cross-section vanishes. This leads to the condition $A_{12} = 0$ and h_0 as follows

$$h_0 = \frac{n(R_E - 1)h}{2(n+2)(n+R_E)}, \quad R_E = \frac{E_t}{E_b}. \tag{5}$$

Using notations $\delta T, \delta U$ and $\delta\vartheta$ are the variation of the kinetic energy, the strain energy of the nanobeam and the elastic foundation, respectively, one can write as

$$\begin{aligned}
\delta T &= \int_0^L \left[I_{11}\left(\dot{u}_0\delta\dot{u}_0 + \dot{w}_0\delta\dot{w}_0\right) - I_{12}\left(\dot{u}_0\delta\dot{w}_{0,x} + \dot{w}_{0,x}\delta\dot{u}_0\right) + I_{22}\dot{w}_{0,x}\delta\dot{w}_{0,x}\right]\mathrm{d}x, \\
\delta U &= \int_0^L \left(N\delta u_{0,x} - M\delta w_{0,xx}\right)\mathrm{d}x, \quad \delta\vartheta = \int_0^L \left(K_w w_0\delta w_0 + K_p w_{0,x}\delta w_{0,x}\right)\mathrm{d}x,
\end{aligned} \tag{6}$$

where N and M are the axial normal force and the bending moment, respectively

$$N = \int_A \sigma_{xx} \mathrm{d}A, \quad M = \int_A (z - h_0)\, \sigma_{xx} \mathrm{d}A, \tag{7}$$

K_w, K_p are the stiffness of Pasternak's elastic foundation. Applying Hamilton's principle

$$\delta \mathbf{L} = \delta \int_0^T L \mathrm{d}t = \int_0^T (\delta T - \delta U - \delta \vartheta) \mathrm{d}t = 0,$$

one can get the equations of motion

$$N_{,x} = I_{11} \ddot{u}_0 - I_{12} \ddot{w}_{0,x}, \quad M_{,xx} - K_w w_0 + K_p w_{0,xx} = I_{11} \ddot{w}_0 + I_{12} \ddot{u}_{0,x} - I_{22} \ddot{w}_{0,xx}, \tag{8}$$

and the corresponding boundary conditions

$$u_0 = 0 \text{ or } N = 0,\ w_0 = 0 \text{ or } Q = M_{,x} - I_{12} \ddot{u}_0 + I_{22} \ddot{w}_{0,x} = 0,\ w_{0,x} \text{ or } M = 0. \tag{9}$$

The nonlocal constitutive equations for nanobeams can be written in the form [7]

$$\sigma_{xx} - \mu \sigma_{xx,xx} = E \varepsilon_{xx}, \quad \mu = (e_0 a)^2, \tag{10}$$

where e_0 is a constant of each material; a and l are internal and external characteristic lengths, respectively; $\mu = e_0^2 a^2$ is a nonlocal parameter. Then

$$N - \mu N_{,xx} = A_{11} u_{0,x} - A_{12} w_{0,xx}, \quad M - \mu M_{,xx} = A_{12} u_{0,x} - A_{22} w_{0,xx}. \tag{11}$$

Substituting (11) into Eqs. (8), (9) leads to the equations of vibration

$$\begin{aligned} &A_{11} u_{0,xx} - A_{12} w_{0,xxx} + \mu \left(I_{11} \ddot{u}_{0,xx} - I_{12} \ddot{w}_{0,xxx} \right) - I_{11} \ddot{u}_0 + I_{12} \ddot{w}_{0,x} = 0, \\ &A_{12} u_{0,xxx} - A_{22} w_{0,xxxx} + \mu \left[I_{11} \ddot{w}_{0,xx} + I_{12} \ddot{u}_{0,xxx} - I_{22} \ddot{w}_{0,xxxx} \right] - I_{11} \ddot{w}_0 \\ &- I_{12} \ddot{u}_{0,x} + I_{22} \ddot{w}_{0,xx} - K_w w_0 + K_p w_{0,xx} + \mu \left(K_w w_{0,xx} - K_p w_{0,xxxx} \right) = 0, \end{aligned} \tag{12}$$

and the corresponding natural boundary conditions at the free ends

$$\begin{aligned} N &= A_{11} u_{0,x} - A_{12} w_{0,xx} + \mu \left(I_{11} \ddot{u}_{0,x} - I_{12} \ddot{w}_{0,xx} \right) = 0, \\ M &= -\left(A_{22} + \mu K_p \right) w_{0,xx} + A_{12} u_{0,x} + \mu \left(I_{11} \ddot{w}_0 + I_{12} \ddot{u}_{0,x} - I_{22} \ddot{w}_{0,xx} + K_w w \right) = 0, \\ Q &= -\left(A_{22} + \mu K_p \right) w_{0,xxx} + A_{12} u_{0,xx} + \mu \left(I_{11} \ddot{w}_{0,x} + I_{12} \ddot{u}_{0,xx} - I_{22} \ddot{w}_{0,xxx} + K_w w'_x \right) \\ &\quad - I_{12} \ddot{u}_0 + I_{22} \ddot{w}_{0,x} = 0. \end{aligned} \tag{13}$$

It can be shown that the nonlocal equations (12) with the boundary conditions (13) are not self-adjoint for nanostructures with free ends. It is worth noting that the resultants in the expressions (13) are not variational–consistent. To overcome this nonlocal paradox, the weak form of differential equations is obtained by multiplying Eqs. (12) by $\delta u_0, \delta w_0$, respectively

$$
\begin{aligned}
0 = & \int_{t_0}^{t_1}\int_{0}^{L}\left[A_{11}u_{0,xx} - A_{12}w_{0,xxx} - I_{11}\ddot{u}_0 + I_{12}\ddot{w}_{0,x} + \mu\left(I_{11}\ddot{u}_{0,xx} - I_{12}\ddot{w}_{0,xxx}\right)\right]\delta u_0 \mathrm{d}x\mathrm{d}t \\
& + \int_{t_0}^{t_1}\int_{0}^{L}\left[\begin{array}{l} A_{12}u_{0,xxx} - A_{22}w_{0,xxxx} - I_{11}\ddot{w}_0 - I_{12}\ddot{u}_{0,x} + I_{22}\ddot{w}_{0,xx} \\ +\mu\left(I_{11}\ddot{w}_{0,xx} + I_{12}\ddot{u}_{0,xxx} - I_{22}\ddot{w}_{0,xxxx}\right) \\ -K_w w_0 + K_p w_{0,xx} + \mu\left(K_w w_{0,xx} - K_p w_{0,xxxx}\right)\end{array}\right]\delta w_0 \mathrm{d}x\mathrm{d}t.
\end{aligned}
\tag{14}
$$

Integrating by parts, the weak form of Eqs. (12) is rewritten as follows

$$
\begin{aligned}
0 = & \int_{t_0}^{t_1}\int_{0}^{L}\left[\delta T - \delta U - \delta\vartheta\right]\mathrm{d}x\mathrm{d}t + \int_{t_0}^{t_1}\left[N\delta u_0 + M\delta w_{0,x} + Q\delta w_0\right]\Big|_0^L \mathrm{d}t \\
& + \int_{0}^{L}\left[\begin{array}{l}\left(-I_{11}\dot{u}_0 + \mu I_{11}\dot{u}_{0,xx} + I_{12}\dot{w}_{0,x} - \mu I_{12}\dot{w}_{0,xxx}\right)\delta u_0 + \\ \left(-I_{12}\dot{u}_{0,x} + \mu I_{12}\dot{u}_{0,xxx} - I_{11}\dot{w}_0 + \mu I_{11}\dot{w}_{0,xx} + I_{22}\dot{w}_{0,xx} - \mu I_{22}\dot{w}_{0,xxxx}\right)\delta w_0\end{array}\right]\Big|_{t_0}^{t_1}\mathrm{d}x \\
& + \left[\left(-\mu I_{11}\dot{u}_{0,x} + \mu I_{12}\dot{w}_{0,xx}\right)\delta u_0 + \left(-\mu I_{12}\dot{u}_{0,xx} - \mu I_{11}\dot{w}_{0,x} - I_{22}\dot{w}_{0,x} + \mu I_{22}\dot{w}_{0,xxx}\right)\delta w_0\right]\Big|_{t_0}^{t_1}\Big|_0^L,
\end{aligned}
\tag{15}
$$

where

$$
\begin{aligned}
N &= A_{11}u_{0,x} - A_{12}w_{0,xx} + \mu\left(I_{11}\ddot{u}_{0,x} - I_{12}\ddot{w}_{0,xx}\right), \\
M &= \left(A_{22} + \mu K_P\right)w_{0,xx}, \\
Q &= A_{12}u_{0,xx} + \mu I_{12}\ddot{u}_{0,xx} + \left(K_P + \mu K_w\right)w_{0,x} - \left(A_{22} + \mu K_P\right)w_{0,xxx} \\
&\quad + \mu I_{11}\ddot{w}_{0,x} + I_{22}\ddot{w}_{0,x} - \mu I_{22}\ddot{w}_{0,xxx}.
\end{aligned}
\tag{16}
$$

The variational-consistent boundary conditions are obtained as

$$
\begin{aligned}
& u_0 = 0 \text{ or } A_{11}u_{0,x} - A_{12}w_{0,xx} + \mu\left(I_{11}\ddot{u}_{0,x} - I_{12}\ddot{w}_{0,xx}\right) = 0, \\
& w_{0,x} = 0 \text{ or } \left(A_{22} + \mu K_P\right)w_{0,xx} = 0, \\
& w_0 = 0 \text{ or } A_{12}u_{0,xx} + \mu I_{12}\ddot{u}_{0,xx} + \left(K_P + \mu K_w\right)w_{0,x} - \left(A_{22} + \mu K_P\right)w_{0,xxx} \\
& \qquad + \mu I_{11}\ddot{w}_{0,x} + I_{22}\ddot{w}_{0,x} - \mu I_{22}\ddot{w}_{0,xxx} = 0.
\end{aligned}
\tag{17}
$$

Eq. (15) provides all possible boundary conditions of the Euler-Bernoulli nanobeam. The boundary conditions (17) are self-adjoint. Moreover, the boundary conditions (17) are identical to the boundary conditions (13) for clamped, clamped-simply and simply supported ends. So in the following only framed nanostructures with free ends are studied.

Setting

$$
\left\{U, W\right\} = \int_{-\infty}^{\infty}\left\{u_0(x,t), w_0(x,t)\right\}e^{-i\omega t}\mathrm{d}t,
\tag{18}
$$

and using the matrices and vectors

$$[\mathbf{A}_0] = \begin{pmatrix} 0 & 0 \\ 0 & A_{22} - \mu\left(I_{22}\omega^2 - K_p\right) \end{pmatrix}, \; [\mathbf{A}_1] = \begin{pmatrix} 0 & -\left(A_{12} - \mu I_{12}\omega^2\right) \\ -\left(A_{12} - \mu I_{12}\omega^2\right) & 0 \end{pmatrix},$$
$$[\mathbf{A}_2] = \begin{pmatrix} A_{11} - \mu I_{11}\omega^2 & 0 \\ 0 & I_{22}\omega^2 - K_p + \mu\left(I_{11}\omega^2 - K_w\right) \end{pmatrix},$$
$$[\mathbf{A}_3] = \begin{pmatrix} 0 & -I_{12}\omega^2 \\ -I_{12}\omega^2 & 0 \end{pmatrix}, \; [\mathbf{A}_4] = \begin{pmatrix} I_{11}\omega^2 & 0 \\ 0 & -\left(I_{11}\omega^2 - K_w\right) \end{pmatrix}, \; \{\mathbf{z}\} = \begin{Bmatrix} U \\ W \end{Bmatrix}, \tag{19}$$

then Eqs. (12) now can be described in the form of

$$[\mathbf{A}_0]\left\{\frac{\mathrm{d}^4\mathbf{z}}{\mathrm{d}x^4}\right\} + [\mathbf{A}_1]\left\{\frac{\mathrm{d}^3\mathbf{z}}{\mathrm{d}x^3}\right\} + [\mathbf{A}_2]\left\{\frac{\mathrm{d}^2\mathbf{z}}{\mathrm{d}x^2}\right\} + [\mathbf{A}_3]\left\{\frac{\mathrm{d}\mathbf{z}}{\mathrm{d}x}\right\} + [\mathbf{A}_4]\{\mathbf{z}\} = \{\mathbf{0}\}. \tag{20}$$

Choosing the solutions of Eqs. (20) in the form of $\{\mathbf{z}_0\} = \{\mathbf{d}\}e^{\lambda x}$ leads to

$$\left(\lambda^4[\mathbf{A}_0] + \lambda^3[\mathbf{A}_1] + \lambda^2[\mathbf{A}_2] + \lambda[\mathbf{A}_3] + [\mathbf{A}_4]\right)\{\mathbf{d}\} = \{\mathbf{0}\}. \tag{21}$$

Eq. (21) has non-zero solutions when the determinant is equal to 0. Expanding these equations, we receive cubic equations of $\eta = \lambda^2$

$$a\eta^3 + b\eta^2 + c\eta + d = 0, \tag{22}$$

where

$$\begin{aligned} a &= \mu^2\left[\left(I_{11}I_{22} - I_{12}^2\right)\omega^4 - I_{11}K_p\omega^2\right] - \mu\left[\left(A_{11}I_{22} - 2A_{12}I_{12} + A_{22}I_{11}\right)\omega^2 - A_{11}K_p\right] \\ &\quad + A_{11}A_{22} - A_{12}^2, \\ b &= -\mu\left[2\left(I_{11}I_{22} - I_{12}^2\right) + \mu I_{11}^2\right]\omega^4 + \left\{\mu^2 I_{11}K_w + \mu\left[\left(2k_p + A_{11}\right)I_{11}\right]\right. \\ &\quad \left. + A_{11}I_{22} - 2A_{12}I_{12} + A_{22}I_{11}\right\}\omega^2 - \mu A_{11}K_w - A_{11}K_p, \\ c &= \left(I_{11}I_{22} - I_{12}^2 + 2\mu I_{11}^2\right)\omega^4 - \left[A_{11} + K_p + 2\mu K_w I_{11}\right]\omega^2 + A_{11}K_w, \\ d &= -I_{11}\omega^2\left(I_{11}\omega^2 - K_w\right). \end{aligned} \tag{23}$$

The solutions of these cubic equations (22) are $\eta_1(\omega), \eta_2(\omega), \eta_3(\omega)$. Using notations

$$\lambda_{1,4} = \pm k_1, \quad \lambda_{2,5} = \pm k_2, \quad \lambda_{3,6} = \pm k_3, \quad k_j = \sqrt{\eta_j}, \quad j = 1,2,3 \tag{24}$$

$$\alpha_1 = k_1\frac{\left(A_{12} - \mu I_{12}\omega^2\right)k_1^2 + I_{12}\omega^2}{\left(A_{11} - \mu I_{11}\omega^2\right)k_1^2 + I_{11}\omega^2 - K_w} = -\alpha_4. \tag{25}$$

Similarly, $\alpha_2 = -\alpha_5, \alpha_3 = -\alpha_6$, the general solutions of Eqs. (20) are in the form as follows

$$\{\mathbf{z}_0(x,\omega)\} = [\mathbf{\Psi}]\{\mathbf{C}\}, \tag{26}$$

where $\{\mathbf{C}\} = (C_1, ..., C_6)^T$ is a constant vector, $\mathbf{\Psi}$ is the function matrix

$$\mathbf{\Psi} = \begin{bmatrix} \alpha_1 e^{k_1 x} & \alpha_2 e^{k_2 x} & \alpha_3 e^{k_3 x} & -\alpha_1 e^{-k_1 x} & -\alpha_2 e^{-k_2 x} & -\alpha_3 e^{-k_3 x} \\ e^{k_1 x} & e^{k_2 x} & e^{k_3 x} & e^{-k_1 x} & e^{-k_2 x} & e^{-k_3 x} \end{bmatrix}. \tag{27}$$

Setting

$$\{\tilde{\mathbf{z}}_0(x,\omega)\} = \left\{U(x,\omega); W'(x,\omega); W(x,\omega)\right\}^T = \left[\hat{\mathbf{\Psi}}\,(x,\omega)\right]\{\mathbf{C}\}. \tag{28}$$

The natural variational-consistent boundary conditions (17) can be rewritten in the form

$$\left\{\begin{array}{ccc} N & M & Q \end{array}\right\}^T = \left[\hat{\mathbf{B}}_{\mathbf{F}}\right]\{\tilde{\mathbf{z}}_0\}, \tag{29}$$

where $\left[\hat{\mathbf{B}}_{\mathbf{F}}\right], \{\tilde{\mathbf{z}}_0\}$ are matrices

$$\left[\hat{\mathbf{B}}_{\mathbf{F}}\right] = \begin{bmatrix} \left(A_{11}-\mu I_{11}\omega^2\right)\partial_x & -\left(A_{12}-\mu I_{12}\omega^2\right)\partial_x & 0 \\ 0 & \left(A_{22}+\mu K_p\right)\partial_x & 0 \\ \left(A_{12}-\mu I_{12}\omega^2\right)\partial_x^2 & \left[K_p+\mu K_w-\left(I_{22}+\mu I_{11}\right)\omega^2\right]-\left[A_{22}-\mu I_{22}\omega^2+\mu K_p\right]\partial_x^2 & 0 \end{bmatrix},$$

$$\{\tilde{\mathbf{z}}_0\} = \left\{\begin{array}{c} U \\ W' \\ W \end{array}\right\}. \tag{30}$$

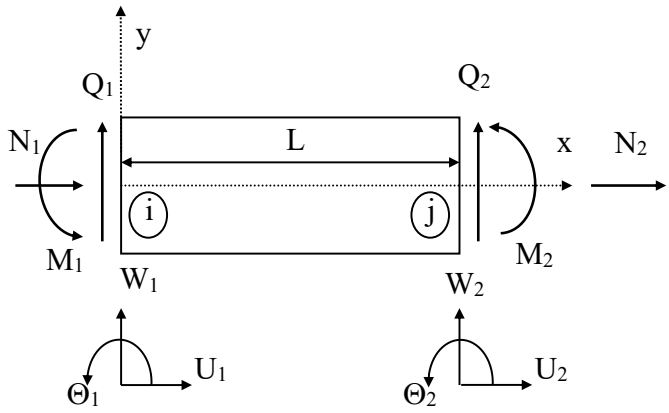

Fig. 2. Nodal displacements and forces of nanobeam element

Consider a FGM nanobeam element with nodal displacements and forces as shown in Fig. 2

$$\{\hat{\mathbf{U}}_e\} = \{U_1, \Theta_1, W_1, U_2, \Theta_2, W_2\}^T, \quad \{\mathbf{P}_e\} = \{N_1, M_1, Q_1, N_2, M_2, Q_2\}^T, \tag{31}$$

where

$$U_1 = U(0,\omega), \Theta_1 = W'(0,\omega), W_1 = W(0,\omega), U_2 = U(L,\omega), \Theta_2 = W'(L,\omega), W_2 = W(L,\omega),$$
$$\left(N_1 \quad M_1 \quad Q_1\right)^T = -\left[\hat{\mathbf{B}}_{\mathbf{F}}\right]\left(U_1 \quad \Theta_1 \quad W_1\right)^T, \quad \left(N_2 \quad M_2 \quad Q_2\right)^T = \left[\hat{\mathbf{B}}_{\mathbf{F}}\right]\left(U_2 \quad \Theta_2 \quad W_2\right)^T. \tag{32}$$

Substituting Eq. (28) into Eq. (32) and eliminating vector $\{\mathbf{C}\}$ leads to

$$\{\mathbf{P}_e\} = \left[\hat{\mathbf{K}}_e(\omega)\right].\{\hat{\mathbf{U}}_e\}, \tag{33}$$

where $\left[\hat{\mathbf{K}}_e\right]$ is the *dynamic stiffness matrix* of the FGM nanobeam element

$$[\hat{\mathbf{K}}_e] = \begin{bmatrix} \left[-\hat{\mathbf{B}}_\mathbf{F}\left(\hat{\mathbf{\Psi}}\right)_{x=0}\right] \\ \left[\hat{\mathbf{B}}_\mathbf{F}\left(\hat{\mathbf{\Psi}}\right)_{x=L}\right] \end{bmatrix} \cdot \begin{bmatrix} \left[\hat{\mathbf{\Psi}}(0,\omega)\right] \\ \left[\hat{\mathbf{\Psi}}(L,\omega)\right] \end{bmatrix}^{-1}. \tag{34}$$

For a framed nanostructure, the total dynamic stiffness matrix $\hat{\mathbf{K}}(\omega)$ and the total nodal force vector $\hat{\mathbf{P}}$ can be obtained by balancing the internal forces at every node of the structure. Setting $\hat{\mathbf{U}}$ be the total DOF vector of the structure, the equation of motion of framed structures conducted by the DSM, is

$$\left[\hat{\mathbf{K}}(\omega)\right].\left\{\hat{\mathbf{U}}\right\} = \left\{\hat{\mathbf{0}}\right\}. \tag{35}$$

Therefore, natural frequencies can be found from the following equation

$$\det[\hat{\mathbf{K}}(\omega)] = 0, \tag{36}$$

and the mode shape relating to the natural frequency ω_j is

$$\left\{\varphi_j(x)\right\} = C_j^0 \left[\widehat{\mathbf{G}}\left(x,\omega_j\right)\right]\left\{\hat{\mathbf{U}}_j\right\}, \tag{37}$$

where

$$[\hat{\mathbf{G}}(x,\omega)] = [\mathbf{G}(x,\omega)] \cdot \begin{bmatrix} [\mathbf{G}(0,\omega)] \\ [\mathbf{G}(L,\omega)] \end{bmatrix}^{-1}. \tag{38}$$

3. RESULTS AND DISCUSSION

In this section, firstly, the calculated results are compared with the published results to validate the proposed DSM. Afterwards, the proposed DSM is applied to analyse the influence of the material, geometry, nonlocal, and Pasternak's elastic foundation parameters on the first frequency of FGM-framed nanostructures with free ends.

3.1. Validation

Table 1 shows the calculated results of the nondimensional first frequency $\lambda_1 = \omega_1.L^2.\sqrt{\rho_t A/E_t I}$ of a simply supported homogeneous beam with published results by Reddy [11] according to the Euler–Bernoulli (EBT), the Timoshenko (TBT), the Reddy (RBT) and Levinson (LBT) beam theory. The calculated results using 2 elements are in good approximation (errors under 0.1%) with the analytical solutions of Reddy for different nonlocal parameters $\mu^* = (e_0 a/h)^2$.

Table 2 shows the calculated results of the nondimensional first frequency of a FGM cantilever nanobeam using 2 elements with the published results by Aria and Friswell [26] which used 26 finite elements according to the Timoshenko beam theory. Good agreements (errors $< 1.6\%$) are received for different boundary conditions such as simply

supported ends, clamped - simply supported, and clamped ends. The above comparisons of calculated and published results validate the reliability of the proposed nonlocal DSM.

Table 1. The nondimensional first frequency of a simply supported nanobeam $(L/h = 20)$

μ^*	EBT [11]	TBT [11]	RBT [11]	LBT [11]	Present
0	9.8696	9.8381	9.8381	9.8433	9.8595
0.5	9.6347	9.6040	9.6040	9.6091	9.6248
1.0	9.4159	9.3858	9.3858	9.3908	9.4062
1.5	9.2113	9.1819	9.1819	9.1868	9.2018
2.0	9.0195	8.9907	8.9907	8.9955	9.0102
2.5	8.8392	8.8110	8.8110	8.8156	8.8301
3.0	8.6693	8.6416	8.6416	8.6462	8.6604
3.5	8.5088	8.4816	8.4816	8.4861	8.5001
4.0	8.3569	8.3302	8.3302	8.3347	8.3483
4.5	8.2129	8.1867	8.1867	8.1910	8.2045
5.0	8.0761	8.0503	8.0503	8.0546	8.0678

Table 2. The nondimensional first frequency of a FGM cantilever nanobeam

μ^*	$n = 0.1$		$n = 0.5$		$n = 1$		$n = 2$		$n = 5$	
	[26], (TBT)	Present (EBT)	[26] (TBT)	Present (EBT)	[26] (TBT)	Present (EBT)	[26] (TBT)	Present (EBT)	[26] (TBT)	Present (EBT)
					$L/h = 20$					
0	1.1886	1.1969	1.4052	1.4207	1.5010	1.5205	1.5941	1.6176	1.7169	1.7450
1	1.1818	1.1900	1.3971	1.4125	1.4924	1.5117	1.5850	1.6082	1.7070	1.7349
2	1.1751	1.1832	1.3891	1.4045	1.4839	1.5031	1.5759	1.5991	1.6973	1.7250
3	1.1684	1.1766	1.3813	1.3965	1.4755	1.4946	1.5671	1.5900	1.6878	1.7153
4	1.1619	1.1700	1.3736	1.3887	1.4673	1.4862	1.5583	1.5811	1.6783	1.7057
5	1.1555	1.1635	1.3660	1.3810	1.4592	1.4780	1.5497	1.5724	1.6690	1.6962
					$L/h = 100$					
0	1.1910	1.1975	1.4077	1.4214	1.5036	1.5213	1.5968	1.6183	1.7198	1.7458
1	1.1907	1.1972	1.4074	1.4211	1.5033	1.5209	1.5964	1.6180	1.7194	1.7454
2	1.1904	1.1970	1.4071	1.4208	1.5029	1.5205	1.5960	1.6176	1.7190	1.7450
3	1.1901	1.1967	1.4067	1.4205	1.5026	1.5202	1.5957	1.6173	1.7186	1.7446
4	1.1898	1.1964	1.4064	1.4201	1.5022	1.5198	1.5953	1.6168	1.7182	1.7442
5	1.1896	1.1961	1.4061	1.4198	1.5019	1.5195	1.5949	1.6165	1.7178	1.7438

3.2. Case study

In this subsection, the calculated results for the three first nondimensional frequencies will be presented for two cases:

a) The FGM cantilever nanobeam with geometric and material parameters: $b = h = 1$ nm, $L = 20$ nm, $E_t = 70$ GPa, $\rho_t = 2700$ kg/m^3; $E_b = 393$ GPa, $\rho_b = 3960$ kg/m^3, $v_t = v_b = 0.3$ [24] and Pasternak's elastic foundation coefficients: $k_w = K_w L^4/EI = 0, ..., 40$; $k_p = K_p L^2/EI = 0, ..., 20$ will be studied.

b) The FGM portal nanostructure with clamped-free ends and above geometric, material parameters will be studied.

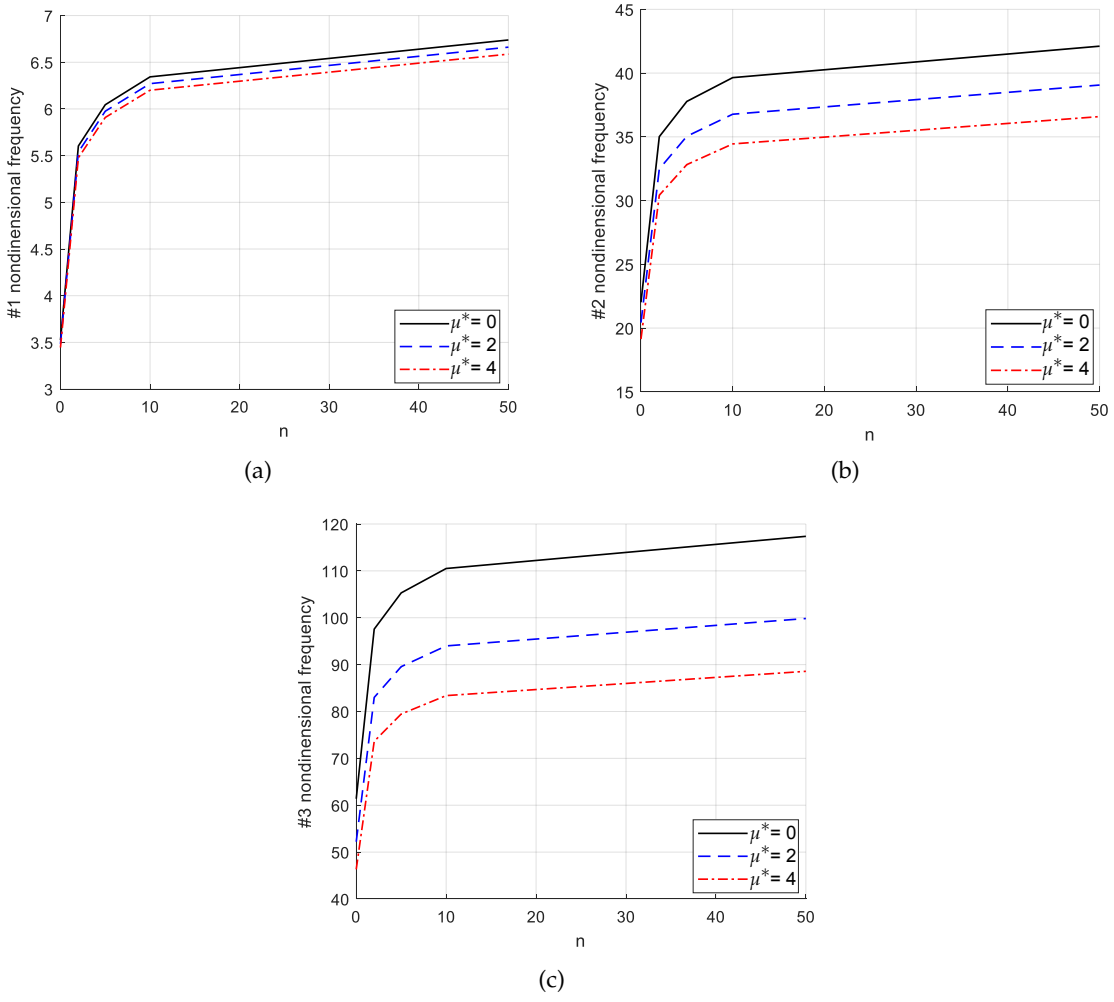

Fig. 3. Changes of first three nondimensional frequencies of the FGM cantilever nanobeam with different nonlocal parameters μ^* and volume fraction indexes n in the case of $L = 20h$ and elastic foundation coefficients $k_w = k_p = 0$

Figs. 3(a)–(c) show the change of three first nondimensional frequencies of the FGM cantilever nanobeam with different nonlocal coefficients μ^* in the case of the length $L = 20h$. Figs. 4(a)–(d) show the change of three first nondimensional frequencies of the FGM portal nanostructure with different nonlocal coefficients μ^* in the case of the length $L = 10h$. Volume fraction indexes are $n = 0, ..., 50$ and elastic foundation coefficients are $k_w = k_p = 0$ in both cases. It is shown that as the volume fraction index increases, there is a significant increase in the nondimensional frequencies, especially when the volume fraction index is under 10. It is noticed that the nonlocal parameter influences the higher frequencies more considerably than the lower ones. The same conclusions are met for the nanobeams and framed nanostructures with other boundary conditions: clamped ends, clamped-free, clamped-simply supported. In the following studies, only cantilever nanobeams are investigated for the sake of simplicity.

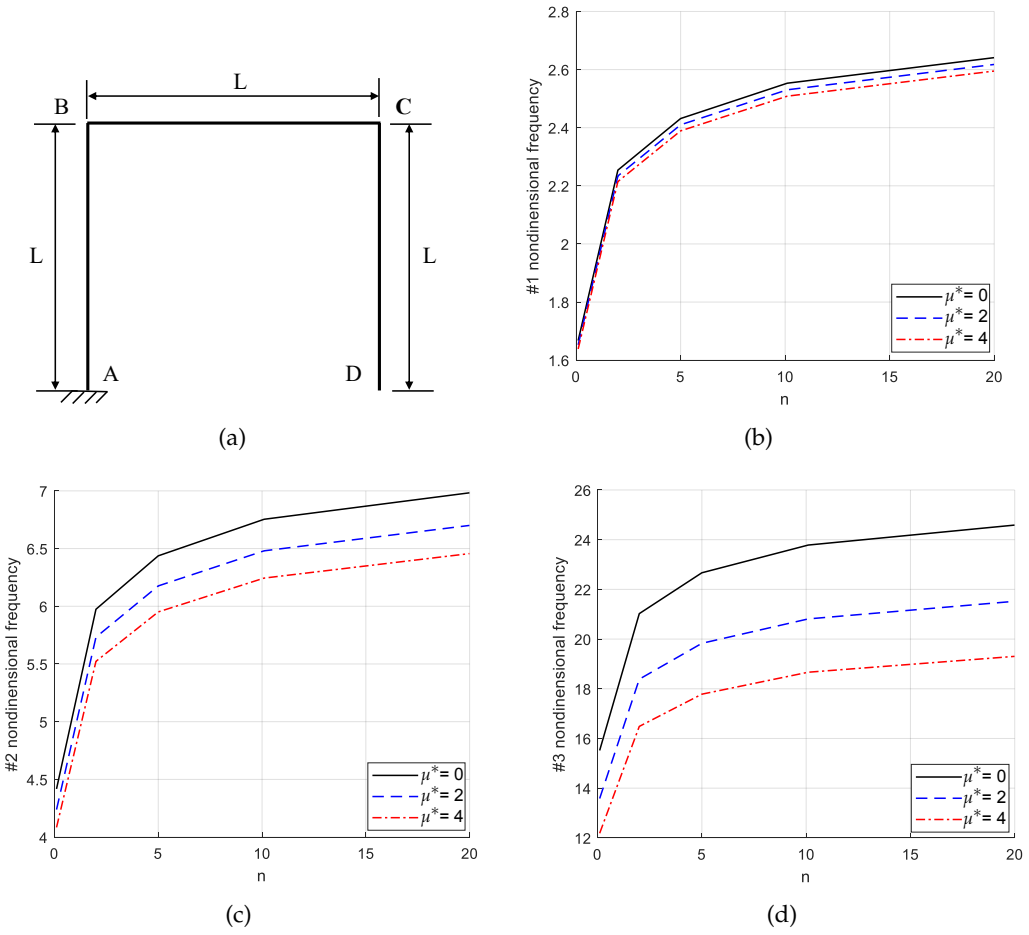

Fig. 4. A portal frame

Figs. 5(a)–(c) show the change of three first nondimensional frequencies of the FGM cantilever nanobeam with different nonlocal coefficients μ^* and ratios $L/h = 20, ..., 100$ in the case of the volume fraction index $n = 2$ and the elastic foundation coefficients $k_w = k_p = 0$. As the ratio L/h increases, there is a significant increase in the nondimensional frequencies, especially when the ratio L/h is in a range of 20-50. It is noticed that the nonlocal parameter influences the higher frequencies more considerably than the lower ones.

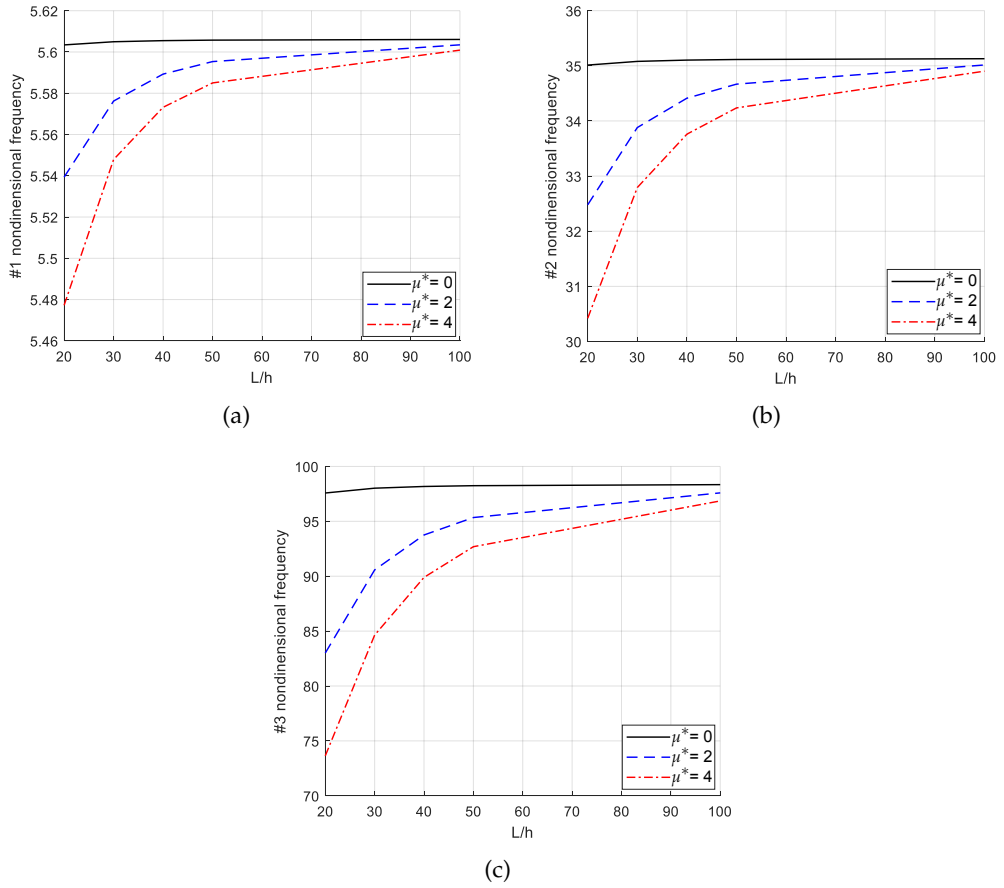

Fig. 5. Change of first three nondimensional frequencies of the FGM cantilever nanobeam with different nonlocal parameters μ^* and ratios L/h in the case of the volume fraction index $n = 2$ and elastic foundation coefficients $k_w = k_p = 0$

Figs. 6(a)–(c) show the change of three first nondimensional frequencies of the FGM cantilever nanobeam with different nonlocal coefficients μ^* and Winkler's elastic foundation coefficients $k_w = 0, ..., 40$ in the case of the length $L = 20h$, the volume fraction index $n = 2$ and the Pasternak's foundation coefficient $k_p = 0$. It is shown that two first

frequencies increase significantly while the third frequency increases slowly. Moreover, the nonlocal parameter influences on the higher frequencies more considerably than the lower ones.

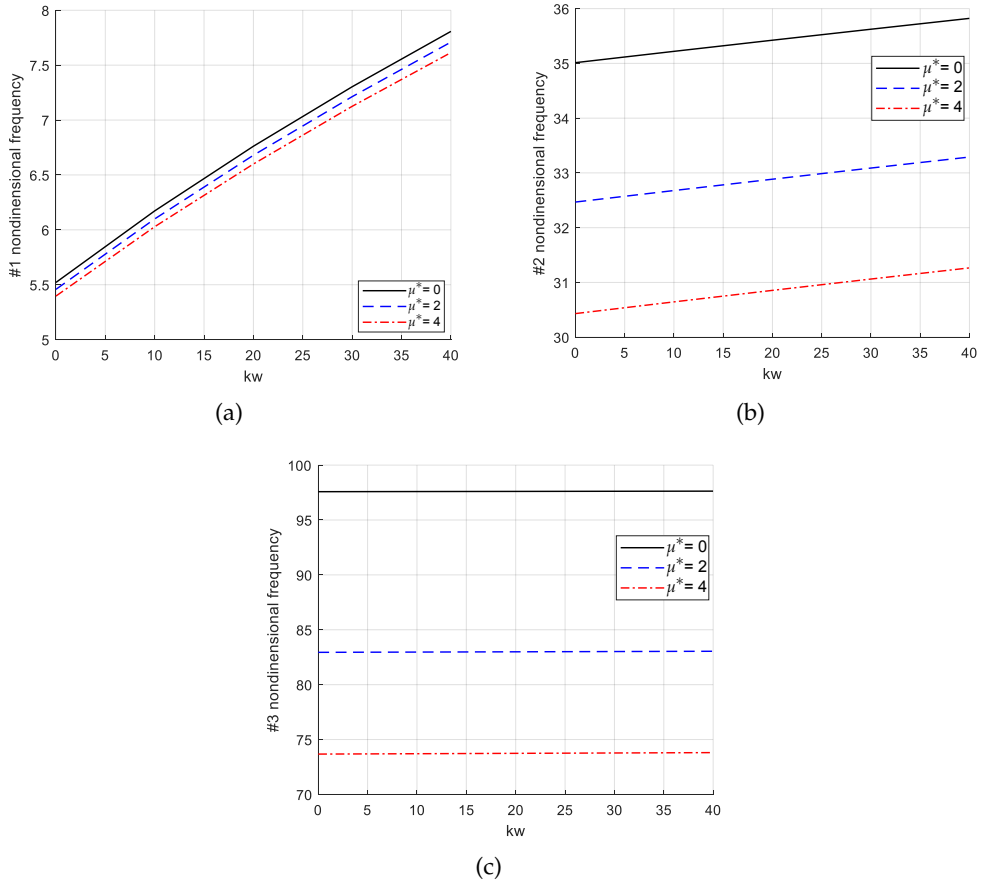

Fig. 6. Changes of first three nondimensional frequencies of the FGM cantilever nanobeam with different nonlocal parameters μ^* and Winkler's elastic foundation coefficients k_w in the case of the volume fraction index $n = 2$ and the Pasternak's foundation coefficient $k_p = 0$

Figs. 7(a)–(c) show the change of three first nondimensional frequencies of the FGM cantilever nanobeam with different nonlocal coefficients μ^* and Pasternak's elastic foundation coefficients $k_p = 0, ..., 20$ in the case of the length $L = 20h$, the volume fraction index $n = 2$ and the Winkler's foundation coefficient $k_w = 0$. As the Pasternak's elastic foundation coefficient increases, there is a significant increase in the nondimensional frequencies. Simultaneously, the nonlocal parameter influences the higher frequencies more considerably than the lower ones.

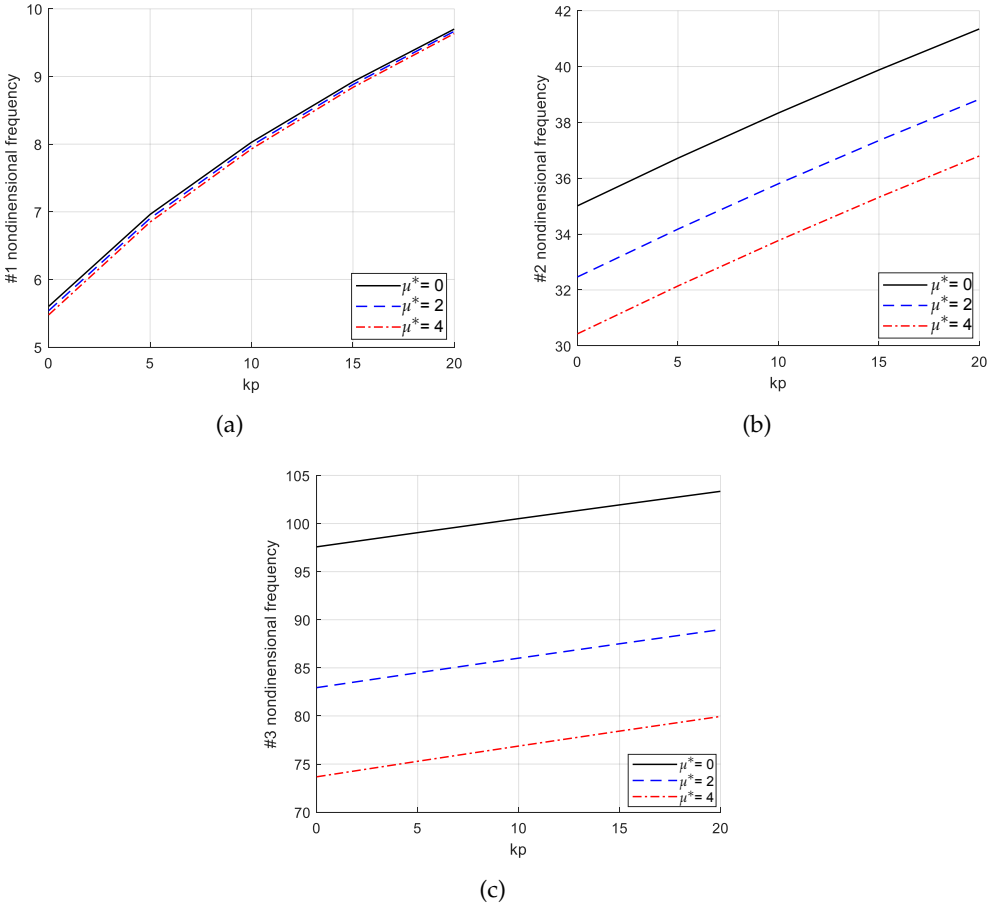

Fig. 7. Changes of first three nondimensional frequencies of the FGM cantilever nanobeam with different nonlocal parameters μ^* and Pasternak's elastic foundation coefficients k_p in the case of the volume fraction index $n = 2$ and the Winkler's elastic foundation coefficient $k_w = 0$

4. CONCLUSIONS

In the present article, a nonlocal DSM is proposed to analyse the free vibration of FGM framed nanostructures on a Pasternak's foundation based on NET and Euler-Bernoulli beam theory. The DSM helps us find exactly the frequencies and mode shapes, especially in the high-frequency range, by using frequency-dependent shape functions that are an exact solution of the vibration problem in the frequency domain. This nonlocal DSM has overcome the stiffening phenomena of the fundamental frequency of nanobeams and nanostructures with the free ends by using the variational-consistent boundary conditions. Comparisons between calculated results and published results validate the reliability of the proposed nonlocal DSM.

The influence of nonlocal, materials, geometric and Pasternak's elastic foundations parameters on the first three nondimensional frequencies of FGM framed nanostructures with free ends is investigated. The calculated results show that the three first nondimensional frequencies of the FGM nanobeam increase significantly when the volume fraction index is under 10 or the ratio L/h is in a range of 20-50. When the elastic foundation coefficient increases, the two first nondimensional frequencies increase significantly while the third frequency increases slowly. In all cases investigated, the nonlocal parameter influences the higher frequencies more considerably than the lower ones.

All the mentioned notices are useful for vibration analysis in FGM framed nanostructures. The study can be applied to more complicated framed nanostructures.

ACKNOWLEDGEMENT

This study was funded by Hanoi University of Civil Engineering under grant number 32-2022/KHXD-TĐ.

DECLARATION OF COMPETING INTEREST

The authors declare that they have no known competing financial interests or personal relationships that could have appeared to influence the work reported in this paper.

REFERENCES

[1] H.-S. Shen. *Functionally graded materials: nonlinear analysis of plates and shells*. CRC Press, (2016).

[2] M. H. Ghayesh and A. Farajpour. A review on the mechanics of functionally graded nanoscale and microscale structures. *International Journal of Engineering Science*, **137**, (2019), pp. 8–36. https://doi.org/10.1016/j.ijengsci.2018.12.001.

[3] A. Farajpour, M. H. Ghayesh, and H. Farokhi. A review on the mechanics of nanostructures. *International Journal of Engineering Science*, **133**, (2018), pp. 231–263. https://doi.org/10.1016/j.ijengsci.2018.09.006.

[4] M. A. Roudbari, T. D. Jorshari, C. Lü, R. Ansari, A. Z. Kouzani, and M. Amabili. A review of size-dependent continuum mechanics models for micro- and nano-structures. *Thin-Walled Structures*, **170**, (2022). https://doi.org/10.1016/j.tws.2021.108562.

[5] V. S. Chandel, G. Wang, and M. Talha. Advances in modelling and analysis of nano structures: a review. *Nanotechnology Reviews*, **9**, (2020), pp. 230–258. https://doi.org/10.1515/ntrev-2020-0020.

[6] A. Garg, H. D. Chalak, A. M. Zenkour, M.-O. Belarbi, and M.-S.-A. Houari. A review of available theories and methodologies for the analysis of nano isotropic, nano functionally graded, and CNT reinforced nanocomposite structures. *Archives of Computational Methods in Engineering*, **29**, (2022), pp. 2237–2270. https://doi.org/10.1007/s11831-021-09652-0.

[7] A. C. Eringen. *Nonlocal continuum field theories*. Springer Science & Business Media, New York, US, (2002).

[8] C. Polizzotto. Nonlocal elasticity and related variational principles. *International Journal of Solids and Structures*, **38**, (2001), pp. 7359–7380. https://doi.org/10.1016/s0020-7683(01)00039-7.

[9] M. A. Eltaher, M. E. Khater, and S. A. Emam. A review on nonlocal elastic models for bending, buckling, vibrations, and wave propagation of nanoscale beams. *Applied Mathematical Modelling*, **40**, (2016), pp. 4109–4128. https://doi.org/10.1016/j.apm.2015.11.026.

[10] H. Salehipour, A. R. Shahidi, and H. Nahvi. Modified nonlocal elasticity theory for functionally graded materials. *International Journal of Engineering Science*, **90**, (2015), pp. 44–57. https://doi.org/10.1016/j.ijengsci.2015.01.005.

[11] J. N. Reddy. Nonlocal theories for bending, buckling and vibration of beams. *International Journal of Engineering Science*, **45**, (2007), pp. 288–307. https://doi.org/10.1016/j.ijengsci.2007.04.004.

[12] C. M. Wang, Y. Y. Zhang, and X. Q. He. Vibration of nonlocal Timoshenko beams. *Nanotechnology*, **18**, (2007). https://doi.org/10.1088/0957-4484/18/10/105401.

[13] C. Li, C. W. Lim, J. L. Yu, and Q. C. Zeng. Analytical solutions for vibration of simply supported nonlocal nanobeams with an axial force. *International Journal of Structural Stability and Dynamics*, **11**, (2011), pp. 257–271. https://doi.org/10.1142/s0219455411004087.

[14] M. Şimşek and H. H. Yurtcu. Analytical solutions for bending and buckling of functionally graded nanobeams based on the nonlocal Timoshenko beam theory. *Composite Structures*, **97**, (2013), pp. 378–386. https://doi.org/10.1016/j.compstruct.2012.10.038.

[15] O. Rahmani and O. Pedram. Analysis and modeling the size effect on vibration of functionally graded nanobeams based on nonlocal Timoshenko beam theory. *International Journal of Engineering Science*, **77**, (2014), pp. 55–70. https://doi.org/10.1016/j.ijengsci.2013.12.003.

[16] I. Mechab, N. E. Meiche, and F. Bernard. Free vibration analysis of higher-order shear elasticity nanocomposite beams with consideration of nonlocal elasticity and poisson effect. *Journal of Nanomechanics and Micromechanics*, **6**, (2016). https://doi.org/10.1061/(asce)nm.2153-5477.0000110.

[17] B. Uymaz. Forced vibration analysis of functionally graded beams using nonlocal elasticity. *Composite Structures*, **105**, (2013), pp. 227–239. https://doi.org/10.1016/j.compstruct.2013.05.006.

[18] M. A. Eltaher, A. E. Alshorbagy, and F. F. Mahmoud. Vibration analysis of Euler–Bernoulli nanobeams by using finite element method. *Applied Mathematical Modelling*, **37**, (2013), pp. 4787–4797. https://doi.org/10.1016/j.apm.2012.10.016.

[19] M. A. Eltaher, F. F. Mahmoud, A. E. Assie, and E. I. Meletis. Coupling effects of nonlocal and surface energy on vibration analysis of nanobeams. *Applied Mathematics and Computation*, **224**, (2013), pp. 760–774. https://doi.org/10.1016/j.amc.2013.09.002.

[20] S. Adhikari, T. Murmu, and M. A. McCarthy. Dynamic finite element analysis of axially vibrating nonlocal rods. *Finite Elements in Analysis and Design*, **63**, (2013), pp. 42–50. https://doi.org/10.1016/j.finel.2012.08.001.

[21] S. C. Pradhan. Nonlocal finite element analysis and small scale effects of CNTs with Timoshenko beam theory. *Finite Elements in Analysis and Design*, **50**, (2012), pp. 8–20. https://doi.org/10.1016/j.finel.2011.08.008.

[22] M. A. Eltaher, A. E. Alshorbagy, and F. F. Mahmoud. Determination of neutral axis position and its effect on natural frequencies of functionally graded macro/nanobeams. *Composite Structures*, **99**, (2013), pp. 193–201. https://doi.org/10.1016/j.compstruct.2012.11.039.

[23] M. A. Eltaher, S. A. Emam, and F. F. Mahmoud. Free vibration analysis of functionally graded size-dependent nanobeams. *Applied Mathematics and Computation*, **218**, (2012), pp. 7406–7420. https://doi.org/10.1016/j.amc.2011.12.090.

[24] M. A. Eltaher, A. A. Abdelrahman, A. Al-Nabawy, M. Khater, and A. Mansour. Vibration of nonlinear graduation of nano-Timoshenko beam considering the neutral axis position. *Applied Mathematics and Computation*, **235**, (2014), pp. 512–529. https://doi.org/10.1016/j.amc.2014.03.028.

[25] M. A. Eltaher, A. Khairy, A. M. Sadoun, and F.-A. Omar. Static and buckling analysis of functionally graded Timoshenko nanobeams. *Applied Mathematics and Computation*, **229**, (2014), pp. 283–295. https://doi.org/10.1016/j.amc.2013.12.072.

[26] A. I. Aria and M. I. Friswell. A nonlocal finite element model for buckling and vibration of functionally graded nanobeams. *Composites Part B: Engineering*, **166**, (2019), pp. 233–246. https://doi.org/10.1016/j.compositesb.2018.11.071.

[27] F. Ebrahimi and P. Nasirzadeh. A nonlocal Timoshenko beam theory for vibration analysis of thick nanobeams using differential transform method. *Journal of Theoretical and Applied Mechanics*, (2015). https://doi.org/10.15632/jtam-pl.53.4.1041.

[28] S. K. Jena and S. Chakraverty. Free vibration analysis of variable cross-section single-layered graphene nano-ribbons (SLGNRs) using differential quadrature method. *Frontiers in Built Environment*, **4**, (2018). https://doi.org/10.3389/fbuil.2018.00063.

[29] O. C. Zienkiewicz, R. L. Taylor, and J. Z. Zhu. *The finite element method: its basis and fundamentals*. Elsevier, (2005).

[30] E. Oñate. *Structural analysis with the finite element method. Linear statics: volume 2: beams, plates and shells*. Springer Science & Business Media, (2013).

[31] H. Su and J. R. Banerjee. Development of dynamic stiffness method for free vibration of functionally graded Timoshenko beams. *Computers & Structures*, **147**, (2015), pp. 107–116. https://doi.org/10.1016/j.compstruc.2014.10.001.

[32] T. V. Lien, N. T. Duc, and N. T. Khiem. Free and forced vibration analysis of multiple cracked FGM multi span continuous beams using dynamic stiffness method. *Latin American Journal of Solids and Structures*, **16**, (2019).

[33] A. Y. T. Leung. *Dynamic stiffness and substructures*. Springer Science & Business Media, (2012).

[34] J. R. Banerjee. Review of the dynamic stiffness method for free-vibration analysis of beams. *Transportation Safety and Environment*, **1**, (2019), pp. 106–116. https://doi.org/10.1093/tse/tdz005.

[35] D. Karličić, T. Murmu, S. Adhikari, and M. McCarthy. *Non-local structural mechanics*. John Wiley & Sons, Inc, (2015).

[36] S. Adhikari, T. Murmu, and M. A. McCarthy. Frequency domain analysis of nonlocal rods embedded in an elastic medium. *Physica E: Low-dimensional Systems and Nanostructures*, **59**, (2014), pp. 33–40. https://doi.org/10.1016/j.physe.2013.11.001.

[37] S. Adhikari, D. Karličić, and X. Liu. Dynamic stiffness of nonlocal damped nanobeams on elastic foundation. *European Journal of Mechanics - A/Solids*, **86**, (2021). https://doi.org/10.1016/j.euromechsol.2020.104144.

[38] M. S. Taima, T. A. El-Sayed, and S. H. Farghaly. Free vibration analysis of multistepped nonlocal Bernoulli–Euler beams using dynamic stiffness matrix method. *Journal of Vibration and Control*, **27**, (2020), pp. 774–789. https://doi.org/10.1177/1077546320933470.

[39] J. Peddieson, G. R. Buchanan, and R. P. McNitt. Application of nonlocal continuum models to nanotechnology. *International Journal of Engineering Science*, **41**, (2003), pp. 305–312. https://doi.org/10.1016/s0020-7225(02)00210-0.

[40] E. Ghavanloo, H. Rafii-Tabar, and S. A. Fazelzadeh. *Computational continuum mechanics of nanoscopic structures*. Springer International Publishing, (2019).

[41] S. Ceballes, K. Larkin, E. Rojas, S. S. Ghaffari, and A. Abdelkefi. Nonlocal elasticity and boundary condition paradoxes: a review. *Journal of Nanoparticle Research*, **23**, (2021). https://doi.org/10.1007/s11051-020-05107-y.

[42] N. Challamel, Z. Zhang, C. M. Wang, J. N. Reddy, Q. Wang, T. Michelitsch, and B. Collet. On nonconservativeness of Eringen's nonlocal elasticity in beam mechanics: correction from a discrete-based approach. *Archive of Applied Mechanics*, **84**, (2014), pp. 1275–1292. https://doi.org/10.1007/s00419-014-0862-x.

[43] P. Khodabakhshi and J. N. Reddy. A unified integro-differential nonlocal model. *International Journal of Engineering Science*, **95**, (2015), pp. 60–75. https://doi.org/10.1016/j.ijengsci.2015.06.006.

[44] Z. Zhang, N. Challamel, and C. M. Wang. Eringen's small length scale coefficient for buckling of nonlocal Timoshenko beam based on microstructured beam model. *Journal of Applied Physics*, **114**, (2013). https://doi.org/10.1063/1.4821246.

[45] J. W. Yan, L. H. Tong, C. Li, Y. Zhu, and Z. W. Wang. Exact solutions of bending deflections for nano-beams and nano-plates based on nonlocal elasticity theory. *Composite Structures*, **125**, (2015), pp. 304–313. https://doi.org/10.1016/j.compstruct.2015.02.017.

[46] X.-J. Xu, Z.-C. Deng, K. Zhang, and W. Xu. Observations of the softening phenomena in the nonlocal cantilever beams. *Composite Structures*, **145**, (2016), pp. 43–57. https://doi.org/10.1016/j.compstruct.2016.02.073.

[47] L. V. Tran, D. B. Tran, and P. T. T. Phan. Free vibration analysis of stepped FGM nanobeams using nonlocal dynamic stiffness model. *Journal of Low Frequency Noise, Vibration and Active Control*, (2023). https://doi.org/10.1177/14613484231160134.